

New Experimental Results Obtained using Microwave Reflectometry in HL-2A Tokamak

W.W. Xiao^{1)*}, X.T. Ding¹⁾, X.L. Zou²⁾, Z.T. Liu¹⁾, Y.D. Gao¹⁾, J.Q. Dong¹⁾, L.H. Yao¹⁾, B.B. Feng¹⁾, X.M. Song¹⁾, S.D. Song²⁾, Y. Zhou¹⁾, C.Y. Chen¹⁾, L.W. Yan¹⁾, Q.W. Yang¹⁾, Yi Liu¹⁾, X.R. Duan¹⁾, C.H. Pan¹⁾, Yong Liu¹⁾

¹Southwestern¹Institute of Physics, P.O. Box 432, Chengdu, China

²Association Euratom-CEA, CEA/DSM/IRFM, CEA/Cadarache, 13018 S'

Paul-lez-Durance, France

1. Introduction

The pulse propagation method is a very powerful tool to study the plasma anomalous transport [1]. To investigate the particle transport in the plasma, the controlled perturbation of the density can be achieved by periodic gas puffing. Gas-feed modulation has been applied in TEXT [2], JT-60U [3]. However, there are some limitations caused by several effects, for example the effect of the recycling, the effect of the nonlinear edge processes, the rapid fall of the amplitude of the perturbation [1]. Especially, the main limitation is the depth of the gas penetration. Therefore, it is very important to use deep and local particle perturbation source for the particle transport study in the core plasma. On HL-1M and HL-2A tokamaks, experiments have been confirmed that the SMBI (Supersonic Molecular Beam Injection) can penetrate more deeply and locally than general gas puffing [4-6]. It seems to be a good perturbation source for particle transport study. The perturbation experiments show that the particle source injected by pulsed MBI is located at $r/a=0.6\sim 0.75$, where the obvious minimum phases can be observed. The maximum amplitude of the first harmonic shifts inward, indicating the presence of an inward convective component. The particle diffusion coefficient and convection velocity during an Ohmic discharge are calculated using an analysis code.

Plasma rotation has been reported in many tokamaks[7, 8]. The plasma rotation profile has been also measured in HL-2A and an new experimental result has been obtained by multi-step Doppler reflectometry system[9]. In purely Ohmic discharge a change of the $\mathbf{E}\times\mathbf{B}$ flow velocity profiles has been observed in the region for $28<r<30\text{cm}$ if the line average density exceeds $2.2\times 10^{19}\text{m}^{-3}$.

2. Experimental results

2.1 Particle transport

The density perturbation source can be induced by the pulsed SMBI in the experiments and the density profile can be measured by scanning microwave reflectometry[10] with a time resolution about 1 ms and spatial resolution less than 1cm. The measurement results show that the amplitude and the phase of the first harmonic for the perturbation density have clear local features. The pulsed molecular beam is injected into the plasma as the density modulation method and the density perturbation source deposition at minor radius can be measured through the scanning microwave reflectometry in HL-2A [10] because of minimum phase profile [1] in HL-2A.

Figure 1 is the measurement results of the density perturbation at the different minor radius during the pulse molecular beam injection. The period of the pulses is 55 ms and gas pressure (P_{SMBI}) is 0.55MPa. The maximal density difference due to the SMBI is $\Delta n_e \approx 2.2\times 10^{18}\text{m}^{-3}$ and the local background plasma density is about $1.5\times 10^{19}\text{m}^{-3}$. So, $\Delta n_e/n_e \approx 14.6\%$ shows that local influence of

* Main author e-mail: xiaoww@swip.ac.cn

the density fluctuation is weaker for the background plasma density.

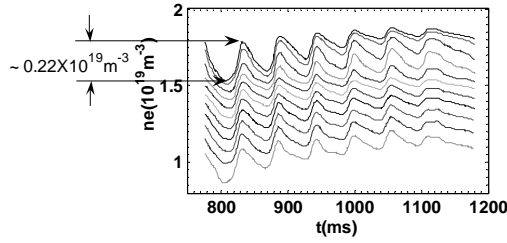


Fig. 1. The density perturbation at different minor radius during the pulse molecular beam injection in shot 3875, $I_p=349$ kA, $B_T=2.3$ T, Gas pressure (P_{SMBI}) =0.55 MPa, from the top down $r=26.5,27,28,29,30,31,32,33,34,35$ and 36 cm.

Different particle source width induces different simulation results. The fittest source width ratio to the experimental results is $w/a = 0.03$, and in the domain A: $D_1=0.2m^2/s$, $V_1= 3m/s$; in the domain B, $D_2=0.4m^2/s$, $V_2=2m/s$ and in the domain C, $D_3=1m^2/s$, $V_3=0.2m/s$ using an analysis model [11]. The profiles of the diffusions D and convection velocities V are shown in Fig. 3. The experiments and the simulations confirm that there are inward particle pinch in the three domains.

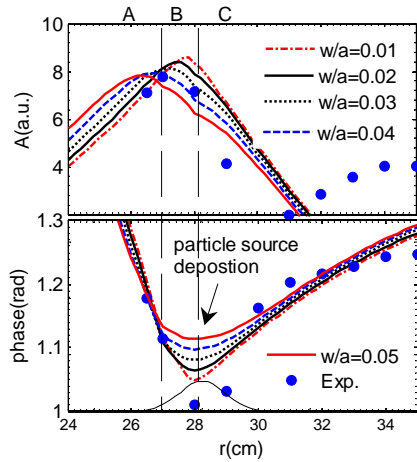


Fig. 2. The experimental and simulations results in different source width, shot 3875.

The particle diffusion coefficients increase with the radius while the inward particle pinch velocities decrease with the radius in this region, $0.6 < r/a < 0.9$.

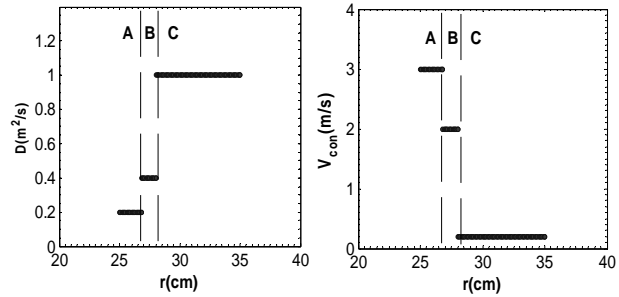
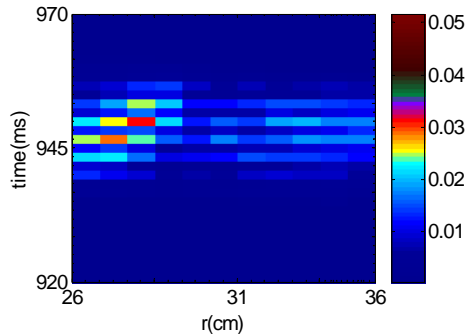


Fig. 3. The diffusion coefficients and the convection velocities profiles in different domains, A,B and C for shot 3875.

In order to confirm the particle source position, the plasma density increase ratio with discharge time has been checked in different radii. This is based on the particle flux balance equation. A assumptive condition is undertaken that the density increase ratio is induced mainly by the particle source. The contour image of the dn_e/dt vs r is shown in Fig. 4. An evidence is that the



plasma density fastly increase as the particle depositions local place, $r \sim 28$ cm. This results agree that the particle source deposition has been measured by the microwave reflectometry as shown in Fig. 2. The error bar means the dn_e/dt value in Fig. 4.

Fig. 4. The contour image of the density variational ratio with discharge time in different radii.

2.2 plasma rotation profile

A broadband sweeping Doppler reflectometry designed for measuring the plasma turbulence is in operation at HL-2A [9, 12]. The main feature of the Doppler reflectometry system is its capability to be tuned, within a fraction of a millisecond, to any selected frequency within the frequency band while keeping synchronized the local and radiofrequency oscillators with the same stability as a fixed frequency system would do. This property enables us to measure several plasma layers within a short time interval during the discharge, permitting characterization of the radial distribution of plasma fluctuations. The system uses the 8 mm fundamental waveguide transmission line and separate antennas for launching and receiving the signal, viewing the plasma from the low field side.

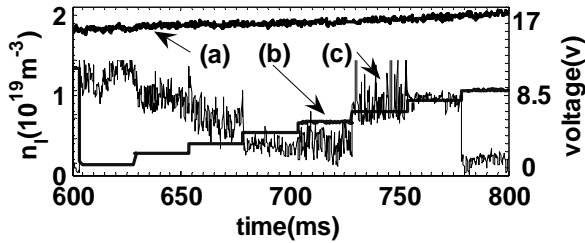
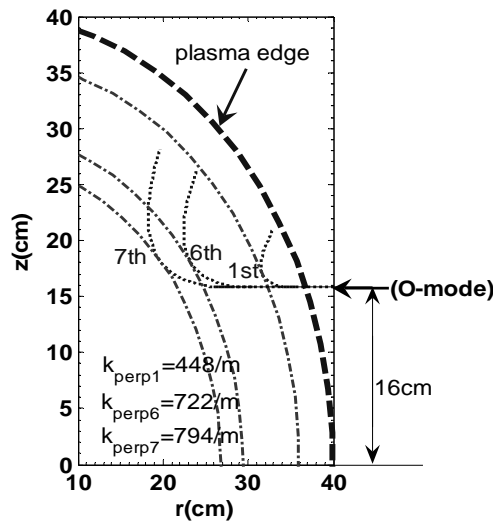


Fig. 5. Time evolution of the line-averaged density for shot 8655. (a) The line average density of $1.9 \times 10^{19} \text{m}^{-3}$. (b) The control voltage for microwave frequency of the Doppler reflectometry system. (c) The initial signal from the Doppler system.

In the current experiments, $E \times B$ flow velocity profile has been measured using the Doppler reflectometry [12]. Time evolution of the line-averaged density is shown for shot 8655. Line average density is about $1.9 \times 10^{19} \text{m}^{-3}$ as shown in Fig. 5(a). Figure 5(b) is the control voltage for microwave frequency of the Doppler reflectometry system. This microwave frequency increases with the control voltage increasing. Figure 5(c) is the initial signal from the

Doppler system with the probing frequencies on different cutoff layers.

Figure 6 shows the results of the ray-trace by REMA code[13] for shot 8614. O-mode (solid line) cutoff surfaces for 26, 35.8 and 37.7 GHz are also shown. There is a distance about 16 cm



between the incidence wave beam and the mid-plane of the device. The dashed curves are ray-tracing predictions from the REMA code. The perpendicular wave numbers k_{perp} can be obtained. The poloidal propagation velocity $V_{E \times B} = \omega/k$ can be calculated and their profiles are shown in Fig. 7.

Fig. 6. Poloidal cross-section showing O-mode (solid line) cut-off surfaces at 26, 35.8 and 37.7 GHz for shot 8614 ($Bt = 1.56T$, $n_l = 2.8 \times 10^{19} \text{m}^{-3}$) with antenna lines of sight. Dashed curves are ray-tracing predictions from REMA code. One can estimate similar circular cross section for the plasma shape.

It has been observed that the $E \times B$ flow velocity profiles are changed if the line average density exceeds $2.2 \times 10^{19} \text{m}^{-3}$. Figure 7(a) shows a continuous increase of the $E \times B$ flow velocity in the range $24 \text{ cm} < r < 36 \text{ cm}$ in shot 8655 (line average density is about $1.9 \times 10^{19} \text{m}^{-3}$) in purely Ohmic discharge. Figures 7(b) and 7(c) present drastic changes of the $E \times B$ flow velocity in the range $28 < r < 30 \text{ cm}$ in shots 8618 (line average

density is about $2.6 \times 10^{19} \text{ m}^{-3}$), and 8614 (line average density is about $2.8 \times 10^{19} \text{ m}^{-3}$). The dashed line shows the position of the velocity change.

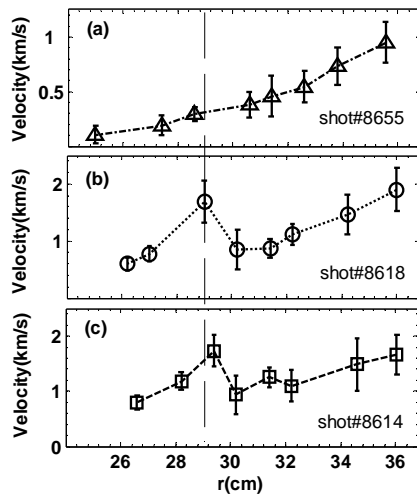


Fig. 7. Radial profiles of the $E \times B$ flow velocity in different line average densities. The $E \times B$ flow velocity increases in the range $24 < r < 36$ cm in shot 8655, line average density is about $1.9 \times 10^{19} \text{ m}^{-3}$. A drastic change of the $E \times B$ flow velocity in the range $28 < r < 30$ cm in shots 8618 ($n_r \sim 2.6 \times 10^{19} \text{ m}^{-3}$), and 8614 ($n_r \sim 2.8 \times 10^{19} \text{ m}^{-3}$). The dashed line shows the position of the velocity change.

3. Summary and discussion

A local particle perturbation source can be formed in plasma confinement region by SMBI. The amplitude and phase profiles of the density perturbations can be obtained after FFT for the data from the microwave reflectometry measurements. The profiles of the amplitude and the phase indicate clear features for the particle transport in HL-2A: the maximum of the amplitude and the minimum of the phase appear in a close area, which is also checked through the density increase ratio on the assumption that the increase ratio is mainly induced by the local neutral particle source; inward particle pinch is observed and the particle diffusion coefficients D and the convection velocities V have been calculated via the simulation analysis model in this way. The plasma rotation profile has been gotten using by the multi-step Doppler reflectometry system in HL-2A. A significant phenomena is that the plasma rotation is related to the plasma density and one special paper to analyse the case using ITG/TEM model[14].

Acknowledgments

The authors are grateful to our colleagues of HL-2A team for their enthusiastic support and valuable discussions. This work is supported by the Natural Science Foundation of China under grant Nos. 10805015 and 10335060.

References

- [1]N.J. Lopes Cardozo, Plasma Phys. Control. Fusion, **37** (1995) 799
- [2]K.W. Gentle et al., Plasma Phys. Control. Fusion, **29** (1987) 1077
- [3]K. Nagashima et al., Nucl. Fusion, **33** (1993) 1677
- [4]Yao Lianghua, et.al., Nucl. Fusion, **38** (1998) 631
- [6]Yao Lianghua et.al., Nucl. Fusion, **41** (2001) 817
- [6]Yao Lianghua et al., Nucl. Fusion, **47** (2007) 1399
- [7]Zou X L, Seak T F, Paume M, et al., 4th Reflectometry Workshop (Cadarache, France, 1999)
- [8]G D Conway, J Schirmer, S Klenge, et al., Plasma Phys. Control. Fusion, **46** (2004) 951
- [9]W.W. Xiao, X.L. Zou, X.T. Ding, et al., Chin. Phys. Lett., **26** (2009) 035201
- [10]W.W.Xiao, Z.T. Liu, X.T. Ding, et al., Plasma Science & Technology, **8** (2006) 133
- [11]S.P. Eury et al., Phys. Plasmas, **12** (2005) 102511
- [12]W.W.Xiao, Ding X T, Liu Z T, et al., Plasma Sci. Technology, **10** (2008) 403
- [13]Krivenski V, Fidone I, Giruzzi G, et al., Nucl. Fusion, **25** (1985) 127
- [14]W.W. Xiao, X.L. Zou, X.T. Ding, to be published, PRL